J. Chem. Eng. Data **1996,** *41,* 831−838

Comparison of High-Pressure Vapor−Liquid Equilibria of Mixtures of CO_2 or Propane with Nonane and C_9 Alkylbenzenes

David W. Jennings and Robert C. Schucker*

Exxon Research and Development Laboratories, Baton Rouge, Louisiana 70821

Vapor−liquid equilibria were measured for (1) binary mixtures of carbon dioxide with nonane, cumene, propylbenzene, or mesitylene, (2) binary mixtures of propane with nonane, cumene, or mesitylene, and (3) ternary mixtures of carbon dioxide, nonane, and cumene. For the carbon dioxide mixtures, vapor−liquid equilibria were measured at 70 °C and at pressures ranging from 3.7 MPa to 12.1 MPa. For the propane mixtures, vapor−liquid equilibria were measured at 104 °C and at pressures ranging from 0.9 MPa to 3.7 MPa. It was found that differences in the phase equilibria of the mixtures could be explained primarily by the self-association of the C_9 components. The composition of the C_9 components in the vapor phase compositions were found to be directly related to the volatility (self-association) of the C_9 component. Liquid phase compositions were found to be enriched in carbon dioxide or propane content in the mixtures containing C_9 compounds having the weakest self-association. Also presented in this paper are comparisons of measurements of vapor−liquid equilibria of carbon dioxide + decane and propane + decane with literature data as validation of the two experimental methods used. These measurements were made at 71 °C for the carbon dioxide + decane mixtures and at temperatures ranging from 38 °C to 120 °C for the propane + decane mixtures.

Introduction

Vapor−liquid equilibria were measured for binary and ternary mixtures comprised of carbon dioxide or propane with nonane, cumene, mesitylene, or propylbenzene. This study was undertaken to provide binary data on these systems (which were unavailable in the literature) while allowing us to validate the performance of newly developed experimental equipment prior to studying more complex mixtures. Previous studies (Dhalewadikar et al., 1987; de Haan and de Graauw, 1992) using supercritical carbon dioxide, ethane, ammonia, $CClF_3$, and CHF_3 were unable to obtain good selectivities for aromatic/saturate separations. These studies revealed that the separations achieved were largely due to volatility differences. Unfortunately, since they dealt with components of widely different volatilities, it is difficult to determine how much effect (if any) the supercritical fluid (SCF) solvent had on the separation. The C_9 components in the present study were chosen due to their similarity in molecular size, volatility, and chemical structure in order to determine (a) if carbon dioxide or propane showed any enhanced solubility for saturated or aromatic compounds and (b) the effect of the various alkyl side chains on the equilibria with the aromatic systems.

Source and Purity of Chemicals

Decane, nonane, cumene (isopropylbenzene), mesitylene (1,3,5-trimethylbenzene), and propylbenzene were obtained from Aldrich Chemical Co. and had stated purities of 99+, 99+, 99, 99, and 98%, respectively. The carbon dioxide was SFC grade (99.999%) and was obtained from Air Products and Chemicals. The propane was obtained from Liquid Carbonics and had a stated purity of 99.99%. All compounds were used without further purification.

Experimental Design and Procedure

The two devices used in this study were developed for making phase equilibrium measurements and for studying applications of supercritical fluid technology to refinery processes. One apparatus contained a variable volume batch cell capable of operating to 200 °C and 30.6 MPa. It was used for determining bubble points, dew points, cloud points, critical points, and three-phase locus points or for observing phase behavior. The second apparatus was a flow apparatus. It was used for the measurement of vapor−liquid, liquid−liquid, and liquid−liquid−vapor equilibria and was capable of operating to 300 °C and 23.1 MPa. It complemented the variable−volume cell in that it allowed determination of coexisting phase compositions.

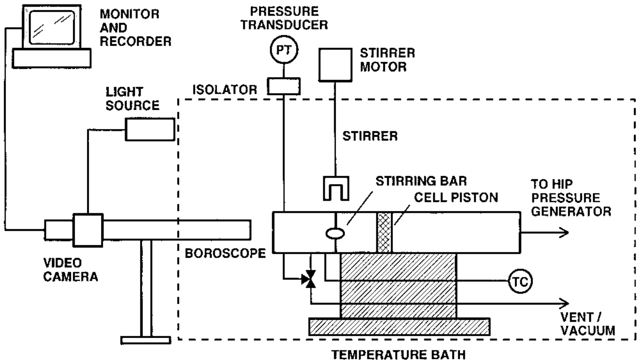

Figure 1. Schematic of variable−volume batch cell apparatus.

Variable−Volume Cell Apparatus. Design. A schematic diagram of the variable−volume cell apparatus is shown in Figure 1. It was similar to that used by McHugh and co-workers (McHugh et al., 1984; Occhiogrosso et al., 1986) and Johnston and co-workers (Lemert et al., 1990; Mawson et al.,1995) for measuring high-pressure vapor−liquid, liquid−liquid, and solid−fluid equilibria, except that different charging procedures were used. The main component of the apparatus was a cylindrical high-pressure cell constructed of stainless steel and equipped with a sapphire window at one end to allow visual observation of fluids under experimental conditions. The inside of the cell contained a piston, which was used to vary the effective volume of the cell, and a fixed Teflon-coated stirring bar to provide mixing. The cell pressure was regulated by the

S0021-9568(96)00033-7 CCC: $12.00

movement of the piston using a working fluid (water) on the backside of the piston pressurized by a HIP pressure generator (Model 87-6-5). The design of the piston provided positive sealing with no leakage of water into the sample. The cell was mounted in a Precision convection oven (Model STG-40) which maintained temperature at ± 1 K of the set point. The temperature was measured by a thermocouple inserted through the cell wall. The pressure was measured by a Schlumberger pressure transducer (Model PG3000-05M-42) connected to an ITT Conflow isolator (Model 140 K). An Autoclave Engineers two stem-three way valve (Model 10V2882) connected to the front of the cell allowed evacuation and charging of the cell and also served as the connection to the pressure transducer/isolator assembly. The phase behavior in the cell was viewed from a video camera/boroscope system (Elmo color camera EC-202II, ITI boroscope series 123000, and ITI light source series 125020/G) connected to a Panasonic medical monitor (Model MT-1340G). Additionally, a video panel monitor (Borland Technology Inc. Model 1200) input the temperature reading, pressure reading, date, and time on the monitor along with the camera images. The camera images and video panel monitor input were recorded on a JVC videocassette recorder (Model HR-FC1000).

Procedure. To begin an experiment, the cell was first evacuated and weighed. Then, the liquid components were charged into the cell from a syringe/valve assembly connected to the cell three way valve. The liquid components could be charged together or separately. After the cell was charged with liquid, it was again evacuated very briefly (to remove any air which entered during charging and to degas the liquid) and weighed to ensure no material had been lost. The last component to be charged was the compressed gas (propane and carbon dioxide in this work). An HIP pressure generator (Model 87-6-5) was used to feed the compressed gas into the cell. The tubing connecting the generator and cell three way valve was evacuated prior to charging in order to prevent any air from entering the cell. The cell was again weighed after charging the compressed gas. Typically, the cell was charged with 12−16 g to ±0.05 g.

Prior to performing a phase equilibrium experiment, the cell and the pressure transducer/isolator were cleaned and pressure tested with nitrogen to ensure no contaminants or leaks were present. If mixtures with solid components were to be studied, a known mass of the solid component(s) was placed in the cell during assembly and then the pressure testing and loading procedure described above was performed.

Next the cell was placed in the oven. The transducer/isolator was connected to the cell three way valve and the backside of the cell was connected to the HIP pressure generator. The transducer/isolator tubing connection was evacuated prior to opening the cell to the transducer/isolator to prevent any air from entering the system. The temperature and pressure were then varied during the course of the experiment to determine phase boundaries. Phase boundaries were determined from visual observation using the video camera/boroscope.

The liquid degassing and cell evacuation after charging the normal liquid components gave no noticeable evaporation loss (for decane) within the precision of our balance (±0.05 g). In fact, evaporative loss of some of the liquid would be of no consequence for binary system measurements since the amount of the liquid component was weighed after the degassing/evacuation. However, if mixtures containing volatile chemicals were to be studied, the degassing procedures employed here could result in evaporation loss which might change the composition of the mixture charged into the cell.

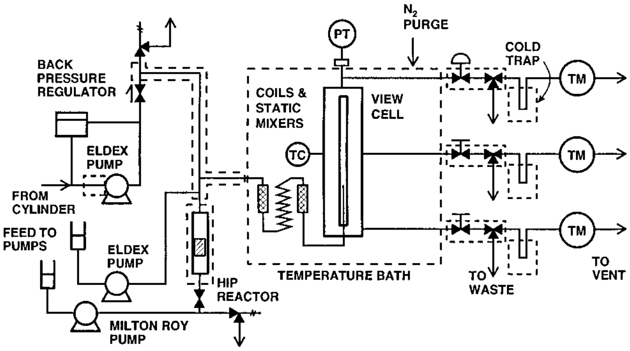

Figure 2. Schematic of flow apparatus.

The pressure transducer/isolator assembly was calibrated against a Beta Products pressure calibrator (Model 320) which was calibrated using standards traceable to the National Institute of Standards and Technology. The pressure measurements were believed to be accurate to within ±20 kPa. The thermocouple was calibrated against an ice bath and checked against vapor pressure measurements of carbon dioxide and propane. The temperature measurements were believed to be accurate to within ±0.2 K. The Mettler balance (Model PC 4400) was calibrated against standard masses, and the mass measurements of the components were believed to be accurate to ±0.1 g.

Flow Apparatus. The flow apparatus used in this work is shown schematically in Figure 2. It was similar in principle to that used by several investigators for measuring high-pressure vapor−liquid equilibria (Simnick et al., 1977; Thies & Paulaitis, 1984; Radosz et al., 1987; Hutchenson et al., 1990; Jennings et al., 1991), yet had several novel features. These included (1) the ability to also measure liquid−liquid−vapor equilibria and (2) the ability to handle systems in which liquid feed components are immiscible. Shown in the schematic is a heated cylinder/piston assembly which adds the capability for pumping heavy components that are very viscous or solid at room temperature. This capability was not used in this work and was simply replaced by a section of tubing. Further explanation is given below.

In flow devices, phase equilibrium is typically established by continuously and thoroughly mixing components at constant temperature during a pumping process. The phases are then separated and analyzed to obtain the equilibrium phase compositions. In this apparatus, up to three metering pumps could be used in making measurements. An Eldex pump (Model B-100-S) was used for pumping a compressed gas from a cylinder. Ice baths over the pump head and around an inlet coil help ensure that the compressed gas remained liquified during pumping. A Milton Roy minipump (Model 92015001) and another Eldex pump were used for pumping normal liquid components (model compounds or petroleum fractions). If the normal liquid feeds are miscible, only one of the pumps was used. If dealing with very viscous or solid materials at room temperature, such as residual oils, the Milton Roy pump metered a working fluid into the heated cylinder (High Pressure Equipment Tubular Reactor, Model TOC15-20) thereby displacing the feed components. This is similar to the design of Hutchenson et al. (1990). Because the feed only contained one nonviscous liquid in this study, only the Eldex pump was used and the tubular reactor was replaced by a section of tubing.

The lines downstream of the pumps and the tubular reactor (if used) were wrapped with heating tape and their temperatures regulated by two mini-Eurotherm temperature controllers (Model 91). This provided preheat prior to the oven and would keep any heavy components (if present) liquified and their viscosity reduced.

All the components were pumped together through a series of static mixers and coils placed within an Applied Test System box oven (Model 3610). The oven maintained a constant temperature environment to ±0.1 K. Phase equilibrium was attained through this section. After equilibration, a Jergenson view cell (Model 19-TCH-40) acted as a phase separator. Up to three phases could be withdrawn; however, the middle phase exit from the view cell was capped and not used in this work. The lower phase was depressurized across a High Pressure Equipment micrometering valve followed by a three way valve. The upper phase was similarly treated except that in some of the experiments the High Pressure Equipment micrometering valve was replaced with a Tescom back-pressure regulator (Model 26-1700). The regulator, micrometering valves, and three way valves were heated to counteract Joule−Thompson cooling effects. The temperatures of the regulator, micrometering valve, and three way valves were maintained by heating tape and Payne variable transformers. The three way valves were used to switch the phases either to a waste collection pot or to sample collection. For sample collection, the condensable portion of each phase was collected in a cold trap, while the noncondensable portion passed through to a gas meter. A Singer wet test meter (Model AL-17-1) was used for most measurements; however, a Singer dry test meter (Model DTM 115-3) was used in some of the experiments for vapor phase measurements. Equilibrium compositions were calculated from the weight of condensable components (subsequent analysis would also be used if more than one condensable component were present) and from the test meter volume measurement of the noncondensable component. Small corrections were made for the noncondensable component dissolved in the condensable components and for the condensable components present in the noncondensable portion leaving the cold trap. An ice bath was used for the lower liquid phase cold trap, while a dry ice + 2-propanol (carbon dioxide mixtures) or dry ice + $CaCl_2$ + water solution (propane mixtures) was used for the vapor phase cold trap.

Constant pressure was maintained by either the back-pressure regulator on the discharge line from the Eldex pump or by the Tescom back-pressure regulator referred to in the previous paragraph. The system pressure was measured to ±20 kPa by a Gould pressure transducer (Model PG3000-05M-42) connected to an ITT Conflow isolator (Model 140 K) with a Chessel digital readout (Model 750). The transducer/isolator assembly was connected to the upper phase leaving the top of the view cell. The tubing leading to the isolator was heated to approximately the oven temperature to prevent condensation of components from the upper phase. The temperature of the tubing was regulated by heating tape and a mini-Eurotherm (Model 91) temperature controller. The system temperature was measured by a thermocouple inserted through the side of the view cell wall. A continuous nitrogen stream (99.99% purity) was introduced into the oven in order to prevent any combustion should a leak develop. The nitrogen flow rate (several liters per minute) was monitored by a Brooks rotameter. The oxygen content of the gas in the oven was not measured separately.

The first step in the experiments was to begin pumping the components to the desired pressure. Next the liquid level was set by adjusting the metering valves and/or pump rates. Analysis of the phases was begun after maintaining steady-state conditions for at least 30 min. Typically, three to four samples of the liquid and vapor phase samples were taken. The phase compositions reported are averages of all the samples. The pressure and temperature were also recorded during the experiment. Although there was little fluctuation in this present work, typically less than 0.1 °C and ±20 kPa, the reported temperatures and pressures are the mean values recorded during the experiments.

Table 1. Bubble Points for Propane (A) + Decane (B)

x_A	t/°C	P/MPa	x_A	t/°C	P/MPa
0.939	37.8	1.234	0.738	37.6	0.958
	50.3	1.620		50.2	1.241
	71.3	2.468		71.4	1.855
	80.2	2.868		80.2	2.151
	104.9	4.289		104.7	3.082
0.891	38.0	1.138		120.1	3.744
	50.2	1.469	0.681	37.8	0.855
	71.3	2.227		50.4	1.138
	80.5	2.627		71.1	1.648
0.872	37.9	1.124		80.1	1.917
	50.2	1.469		104.6	2.744
	71.2	2.179	0.603	37.6	0.758
	80.4	2.558		50.2	0.986
	104.5	3.730		71.2	1.427
	120.3	4.606		80.2	1.641
0.801	37.8	1.041		104.8	2.330
	50.3	1.358		120.8	2.827
	71.4	2.006	0.475	37.8	0.593
	80.4	2.330		50.5	0.758
	104.9	3.378		71.1	1.082
	120.7	4.130		80.5	1.255
0.794	50.6	1.345		104.5	1.724
	71.0	1.999		120.8	2.096
	101.8	3.282			

The pressure transducer/isolator assembly was calibrated against a Beta Products pressure calibrator (Model 320), which was calibrated using standards traceable to the National Institute of Standards and Technology. The pressure measurements are believed to be accurate to within ±20 kPa. The test meters were calibrated against a proving bottle from the American Meter Co. The test meters were found to be accurate to within 0.6%. The thermocouple was calibrated against an ice bath and against the vapor pressure of propane. It is believed to be accurate to within ±0.3 °C.

Results and Discussion on Test System Measurements

Variable−Volume Batch Apparatus (Propane + Decane). Propane + decane bubble point measurements were made at approximately (37.8, 50.3, 71.2, 80.3, 104.7, and 120.5) °C for nine different compositions. The results are presented in Table 1. Some of the compositions are missing measurements at the higher or lower temperatures due to mechanical limitations in the movement of the piston prior to reaching the bubble point.

The results at (37.8, 71.2, and 104.7) °C are presented in Figure 3 along with measurements by Reamer and Sage (1966) at (37.8, 71.1, and 104.4) °C. The data are in good agreement with those by Reamer and Sage although they exhibit some scatter and the measurements at 37.8 °C appear slightly high. The error and scatter are believed to be attributed to two main causes. First, the composition of the cell contents was determined gravimetrically from a Mettler balance (Model PC 4400) which had a resolution of only 0.1 g in the mass range of the cell. For some of the experiments, 0.1 g could represent a significant percentage of the total amount of one of the components charged (up to approximately 5%). Second, it was later found that in

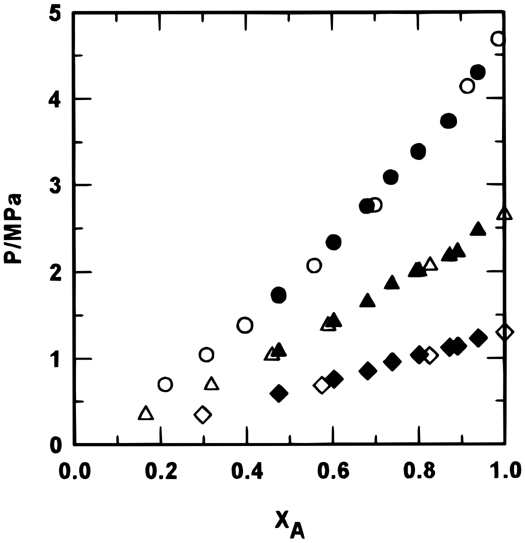

Figure 3. Comparison of bubble point measurements of propane + decane (B) with literature data: (●) this work, 104.7 °C; (○) Reamer and Sage, 104.4 °C; (▲) this work, 71.2 °C; (△) Reamer and Sage, 71.1 °C; (◆) this work, 37.8 °C, (◇) Reamer and Sage, 37.7 °C.

some instances the first bubble in the bubble point measurements came from fluid in the tubing leading to the pressure transducer. Fluid in this dead space may not always be completely mixed or may have a slightly different temperature than the bulk of fluid in the cell. Such a situation is most likely to occur in the first measurements after charging the cell, since generally between measurements at different temperatures the fluid was maintained in a single-phase region to ensure the fluid stayed homogeneous. The 37.8 °C "isotherm" was the first measurement for the propane + decane mixtures and might explain why this isotherm appeared slightly high. For subsequent measurements this source of error was virtually eliminated by simply flushing unmixed fluid out of the tubing leading to the transducer by moving the piston back and forth a few times along with closer observation to ensure the first bubbles did not come solely from tubing leading to the transducer port. Another improvement used in subsequent measurements included better flushing of the three way valve after charging. These improvements reduced the amount of scatter over that present in the propane + decane measurements. The precision limitation of the balance, however, still existed.

Flow Apparatus (Carbon Dioxide + Decane and Propane + Decane). Vapor−liquid equilibrium measurements were made on carbon dioxide + decane mixtures at 71.1 °C as a test for the accuracy of measurements from the apparatus, since a number of investigators (Reamer and Sage, 1963; Nagarajan and Robinson, 1986; Chou et al., 1990) have published results for these mixtures with good agreement among the data sets. Vapor−liquid equilibrium measurements were also made on propane + decane mixtures at 104 °C in order to test the operability of the apparatus with propane, since these measurements required different cold traps for the vapor phase samples. The results also allowed a further check on the accuracy of the measurements from the apparatus since published literature results by Reamer and Sage (1966) for these mixtures exist. The results for carbon dioxide + decane and propane + decane are given in Tables 2 and 3, respectively.

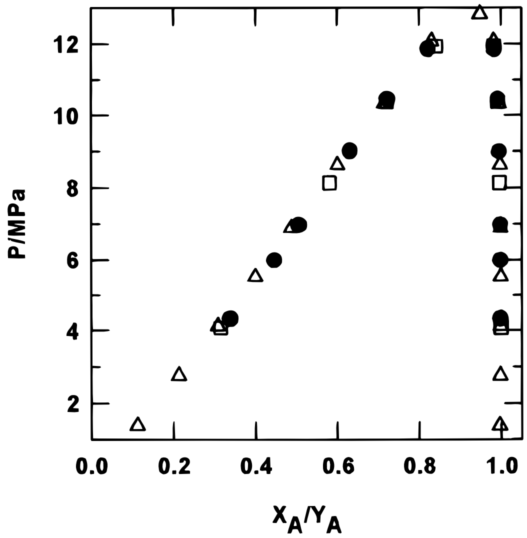

Figure 4. Comparison of vapor−liquid equilibria measurements of carbon dioxide (A) + decane (B) with literature data: (●) this work; (△) Reamer and Sage; (□) Chou et al.

Table 2. Vapor−Liquid Equilibria of Carbon Dioxide (A) + Decane (B)

t/°C	P/MPa	x_A	y_A
71.1	4.330	0.3383	0.9980
71.1	5.964	0.4461	0.9977
71.0	6.964	0.5066	0.9972
71.0	8.977	0.6314	0.9957
71.1	10.446	0.7223	0.9924
71.1	11.852	0.8211	0.9843

Table 3. Vapor−Liquid Equilibria of Propane (A) + Decane (B)

t/°C	P/MPa	x_A	y_A
104.0	0.945	0.2869	0.9844
104.0	1.462	0.4338	0.9909
104.0	1.931	0.5445	0.9922
103.9	2.668	0.6793	0.9924
103.8	3.241	0.7960	0.9931
103.7	3.516	0.8577	0.9940

The vapor−liquid equilibrium measurements for the carbon dioxide + decane system are shown in Figure 4 along with measurements by Reamer and Sage (1963) and Chou et al. (1990). The vapor phase compositions are shown in greater detail in Figure 5. As shown, good agreement exists among the data sets. The reproducibilities of the liquid and vapor phase compositions for the samples were within ±0.0013 and ±0.000 07 mole fraction, respectively.

The vapor−liquid equilibrium measurements for propane + decane at approximately 104 °C are shown in Figure 6 along with the results of Reamer and Sage (1966) at 104.4 °C. The vapor phase compositions are shown in greater detail in Figure 7. Note that the two points at 2.668 and 3.516 MPa are slightly offset from the other points. This is more noticeable in the expanded scale of Figure 7. This was believed to be due to the difference in decane purity, in that these two measurements were made using a bottle of decane from an old supply and all the other measurements were made with recently ordered decane. Nonetheless, even with the slight offset in these two points and taking into account slight temperature differences, good agreement exists between the data sets. The reproducibilities of the liquid and vapor phase compositions were within ±0.0018 and ±0.000 28, respectively. The diminished reproducibility from that of the carbon dioxide + decane measurements was attributed mostly to the pressure control of the experiments. Whereas the pressure control for all the carbon dioxide + decane experiments was

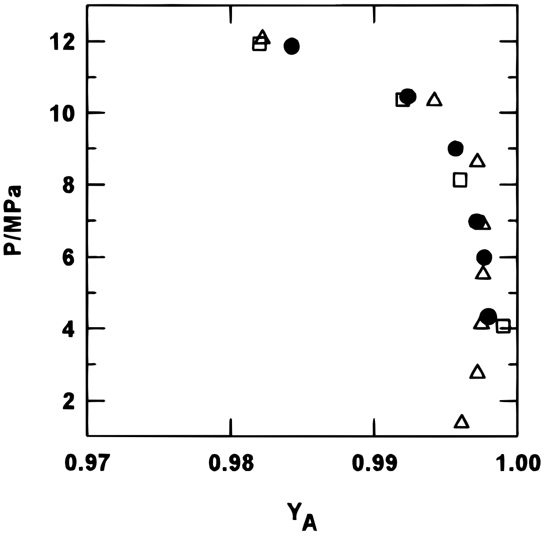

Figure 5. Comparison of vapor−liquid equilibria vapor phase measurements of carbon dioxide (A) + decane (B) with literature data: (●) this work; (△) Reamer and Sage; (□) Chou et al.

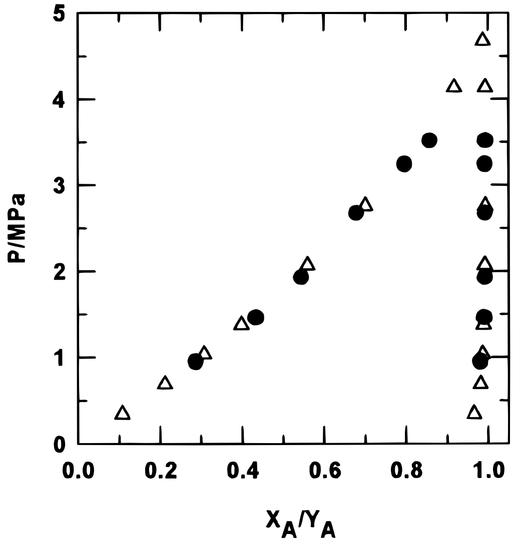

Figure 6. Comparison of vapor−liquid equilibria measurements of propane (A) + decane (B) with literature data: (●) this work;) Reamer and Sage.

generally within ± 7 kPa, the control for some of the propane + decane experiments was only within ± 20 kPa.

No experiments were performed to verify that equilibrium conditions were attained by repeating measurements at different flow rates; however, the flow rates used were in the range of those used by one of the authors previously in experiments in a similar apparatus (Jennings et al., 1991, 1992). Additionally, this apparatus had more tubing than the apparatus used in the previous experiments and an extra static mixer in which the fluids could equilibrate.

Results and Discussion (Binary Mixtures)

As previously mentioned, the various C_9 components were chosen to determine the effect of chemical structure on phase equilibrium. Significant differences exist among the various structures, and therefore, one might expect noticeable differences in the phase equilibria to also exist. The greatest difference, of course, is between the aliphatic structure of nonane and the aromatic structures of the C_9 alkylbenzenes. Less significant, yet appreciable differences also exist between the alkylbenzene structures. Increased molecular interaction in the aromatics is due to (1) resonance stabilization not available in aliphatic molecules and (2) the sharing of electrons through π overlap. Molecular structure significantly affects the latter.

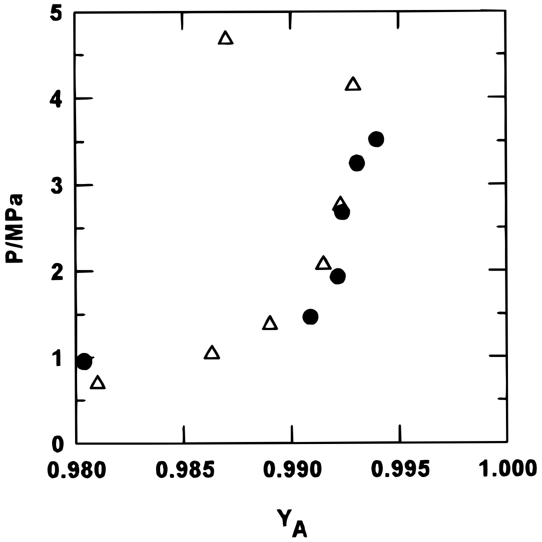

Figure 7. Comparison of vapor−liquid equilibria vapor phase measurements of propane (A) + decane (B) with literature data: (●) this work; (△) Reamer and Sage.

Table 4. Vapor−Liquid Equilibria for Carbon Dioxide (A) + Nonane (B) at 70.1 °C

P/MPa	x_A	y_A
3.730	0.2959	0.9960
5.454	0.4161	0.9957
6.957	0.5173	0.9948
8.556	0.6271	0.9928
10.625	0.7779	0.9859
11.804	0.8829	0.9674

A comparison of the nonane and cumene systems offers a direct measure of the effect that the aromatic and aliphatic structures have on the phase equilibria, since nonane and cumene have similar volatilities. Among the alkylbenzenes, as indicated above, the differences in phase equilibria would be expected to be related more to the self-association of the aromatic rings ($\pi-\pi$ overlap), since the carbon dioxide and propane associations for the various alkylbenzenes would be similar. The relative self-association can be attributed to (a) the effect of the alkyl side chain on the electron density in the ring and (b) the steric hindrance that the alkyl side chain creates. For example, mesitylene with its three methyl groups has the greatest electron density and the lowest steric hindrance. Therefore, it can self-associate more effectively than cumene, which has a lower electron density and significantly greater steric hindrance. One manifestation of these structural differences is the fact that the melting point of mesitylene is 51.3 deg greater than that of cumene. Based on self-association considerations only, interactions of the alkylbenzenes with carbon dioxide or propane would be expected to increase in the order of cumene, *n*-propylbenzene, and mesitylene.

The vapor−liquid equilibrium measurements for the carbon dioxide + nonane, carbon dioxide + cumene, and carbon dioxide + propylbenzene, and carbon dioxide/mesitylene mixtures are presented in Tables 4−7, respectively. Results for the liquid phase compositions for all the mixtures are shown in Figure 8. The liquid phase compositions do show some small differences between aromatic and saturate compounds, as evidenced by the larger difference between the liquid phase compositions for the *n*-nonane and cumene systems than between those for the

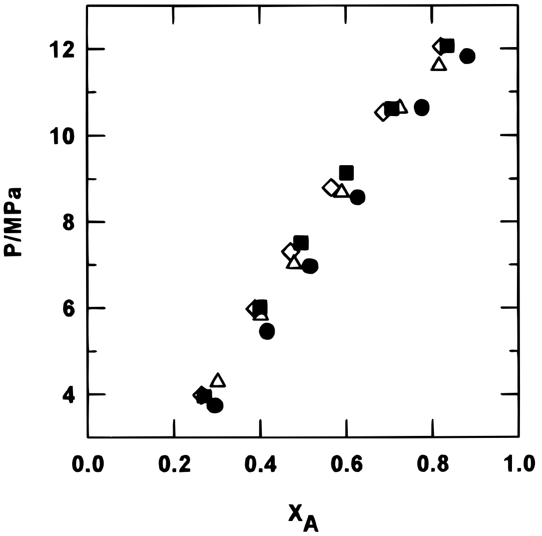

Figure 8. Comparison of vapor phase compositions of various carbon dioxide (A) + C_9 species (B) at 70 °C: (●) nonane; (△) cumene; (■) propylbenzene; (◇) mesitylene.

Table 5. Vapor−Liquid Equilibria for Carbon Dioxide + Cumene (B) at 70.2 °C

P/MPa	x_A	y_A
4.289	0.3009	0.9959
5.833	0.4014	0.9956
7.026	0.4783	0.9948
8.687	0.5888	0.9929
10.625	0.7259	0.9871
11.604	0.8164	0.9776

Table 6. Vapor−Liquid Equilibria for Carbon Dioxide + Propylbenzene (B) at 70.1 °C

P/MPa	x_A	y_A
3.964	0.2699	0.9967
6.026	0.4001	0.9962
7.515	0.4949	0.9952
9.142	0.6010	0.9931
10.618	0.7067	0.9883
12.066	0.8359	0.9724

Table 7. Vapor−Liquid Equilibria for Carbon Dioxide + Mesitylene (B) at 70.1 C

P/MPa	x_A	y_A
3.985	0.2635	0.9972
5.992	0.3884	0.9967
7.315	0.4704	0.9956
8.798	0.5658	0.9939
10.528	0.6860	0.9893
12.059	0.8219	0.9731

alkylbenzene systems. The liquid phase for the nonane mixtures contains more carbon dioxide than the alkylbenzene mixtures as a result of nonane not self-associating as strongly as the alkylbenzenes and, therefore, being able to "hold" more carbon dioxide than the alkylbenzenes. The differences among the alkylbenzene mixtures are consistent with expected behavior when considering the differences in the self-association of the various alkylbenzenes.

Results for the vapor phase for all the systems are shown in Figure 9. The composition of the C_9 compound in the vapor phase is closely related to its volatility (self-associations), no matter whether aromatic or saturate. The vapor phase compositions follow the order of the normal boiling points for *n*-nonane, cumene, propylbenzene, and mesitylene (150.8, 152.4, 159.2, and 169.3 °C [Reid et al. (1987)]) and, in fact, for *n*-nonane and cumene (which have very similar vapor pressures) are almost identical. This seems to indicate that at the vapor phase density no enhanced chemical interactions with the aromatic or saturate molecules occur with carbon dioxide. Also at this fluid density and composition, self-associations of the C_9 are probably not as appreciable.

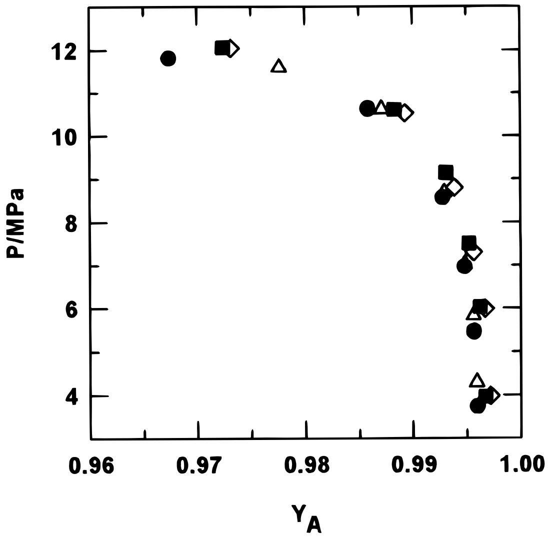

Figure 9. Comparison of liquid phase compositions of various carbon dioxide (A) + C_9 species (B) at 70 °C: (●) nonane; (△) cumene; (■) propylbenzene; (◇) mesitylene.

Table 8. Vapor−Liquid Equilibria for Propane (A) + Nonane (B)

t/°C	P/MPa	x_A	y_A
104.0	0.938	0.2936	0.9739
104.0	1.365	0.4069	0.9810
103.9	2.227	0.6113	0.9868
103.7	3.027	0.7749	0.9893
103.6	3.468	0.8543	0.9904

Table 9. Vapor−Liquid Equilibria for Propane (A) + Cumene (B)

t/°C	P/MPa	x_A	y_A
104.2	1.407	0.3334	0.9808
104.0	2.151	0.5052	0.9853
103.9	2.951	0.6945	0.9881
103.7	3.634	0.8561	0.9896

There appears to be some small increase in interaction of nonane over that of the alkylbenzenes with carbon dioxide in the liquid phase. However, since vapor phase loadings are low and the compositions of saturate and aromatics in the vapor phase are almost identical (with similar volatilities), no large selectivities would be expected in supercritical carbon dioxide extraction. In fact, the few previously reported aromatic/saturate separation studies by supercritical extraction with carbon dioxide have not proven to be very selective [Dhalewadikar et al. (1987) and de Haan and de Graauw (1992)].

The reproducibilities of these liquid and vapor phase compositions were generally within ±0.002 and ±0.000 15 mole fraction, respectively. For these measurements, pressure control was generally within ±1 psi.

The vapor−liquid equilibrium measurements for the propane/*n*-nonane, propane/cumene, and propane/mesitylene mixtures are presented in Tables 8−10, respectively. The liquid and vapor phase compositions for all the systems are shown in Figures 10 and 11, respectively. The phase behavior exhibited is analogous to that of the carbon dioxide mixtures. The liquid phase compositions, like the carbon dioxide mixtures, show a small difference between the aromatic and saturate compounds; and the differences between the alkylbenzene mixtures follow what one would

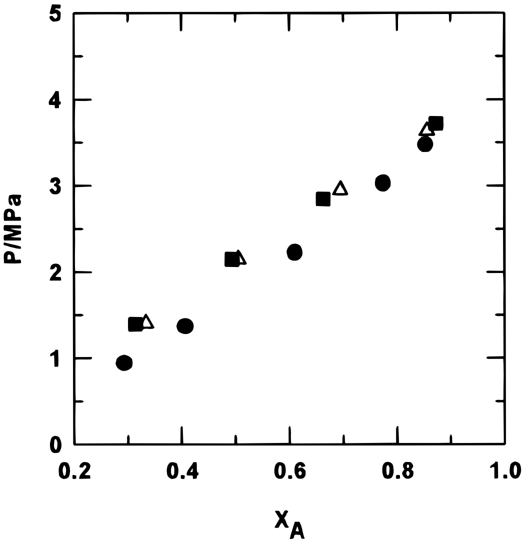

Figure 10. Comparison of liquid phase compositions of various propane (A) + C_9 species (B) at 104 °C: (●) nonane; (△) cumene;) mesitylene.

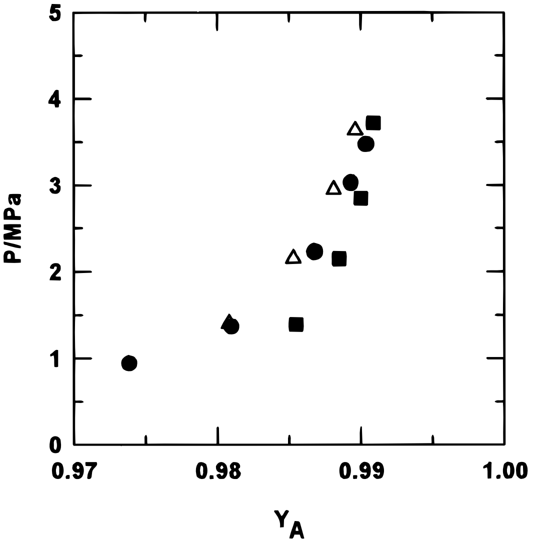

Figure 11. Comparison of vapor phase compositions of various propane (A) + C_9 species (B) at 104 °C: (●) nonane; (△) cumene;) mesitylene.

Table 10. Vapor−Liquid Equilibria for Propane (A) + Mesitylene (B)

t/°C	P/MPa	x_A	y_A
104.1	1.393	0.3139	0.9855
104.1	2.151	0.4937	0.9885
103.8	2.848	0.6631	0.9900
103.7	3.723	0.8733	0.9909

expect on the basis of the differences in self-association of the various alkylbenzenes. The vapor phase composition again is directly related to the C_9 component volatility, whether aromatic and saturate. One slight difference between the carbon dioxide and propane systems is that the C_9 vapor phase composition in the propane systems is slightly greater for cumene than for nonane.

Some small error is present for measurements above 2.5 MPa for each of the systems due to disturbances in the equilibrium conditions. These errors are attributed directly to the pressure control which was generally within ±3 psi for these measurements. Some slight flashing in the liquid phase was observed with these small pressure fluctuations. No condensation was observed from the vapor phase with the pressure drops since, for the pressure range of these measurements, the vapor compositions at lower pressures are higher in the C_9 component. The propane flashed from the liquid phase would, however, also cause an error in the vapor phase measurement as a result of extra propane present in the vapor sample. The lower temperatures for the measurements at higher pressures are undoubtedly a result of the slight flashing due to evaporative cooling in the view cell. The magnitude of the errors in the reported phase compositions is believed to be small since the flashing was slight and a result of differences in equilibrium conditions varying only ±20 kPa.

The reproducibilities of the liquid and vapor phase compositions for these measurements were generally within ±0.002 and ±0.0003 mole fraction, respectively.

Table 11. Bubble Points for Carbon Dioxide (A) + Nonane (B) + Cumene (C) (Nonane/Cumene Mass Ratio of 45/55)

x_A	x_B	t/°C	P/MPa
0.782	0.094	30.3	5.923
		49.9	8.356
		70.1	11.080
		89.9	13.590
		110.2	15.692
0.604	0.172	40.1	5.826
		50.3	6.750
		69.9	8.549
		90.0	10.349
		110.1	11.976
0.587	0.179	40.3	5.723
		50.3	6.578
		70.0	8.329
		90.1	10.025
		110.2	11.597

Table 12. Bubble Points for Carbon Dioxide (A) + Nonane (B) + Cumene (C) (Nonane/Cumene Mass Ratio of 78/22)

x_A	x_B	t/°C	P/MPa
0.781	0.169	30.3	5.874
		50.0	8.219
		70.1	10.742
		89.9	13.072
		110.1	15.017
0.886	0.087	30.2	6.316
		50.2	9.046
		69.9	11.907
0.944	0.043	30.2	6.571
		49.9	9.377
		70.1	12.018

Results and Discussion (Ternary Systems)

Bubble points of carbon dioxide/*n*-nonane/cumene mixtures were measured in the variable−volume apparatus at temperatures between 30 and 80 °C for two fixed nonane/cumene weight ratios of (45/55) and (78/22). The results are given in Tables 11 and 12. In these experiments, carbon dioxide mole fractions ranged from 0.587−0.782 and 0.781−0.944 for the two respective nonane + cumene mixtures. Bubble point measurements for these mixtures were found to be consistent with data from the binary carbon dioxide + nonane and carbon dioxide + cumene mixtures. The bubble point pressures lie between the binary measurements, and the mixtures with the lower nonane/cumene ratio exhibit slightly lower bubble point pressures (less self-association due to less cumene and therefore more interaction with carbon dioxide resulting in higher carbon dioxide compositions). The results of these measurements are shown in Figure 12 along with the vapor−liquid equilibria measurements made on carbon dioxide + nonane and carbon dioxide + cumene binary mixtures at 70 °C in the flow apparatus.

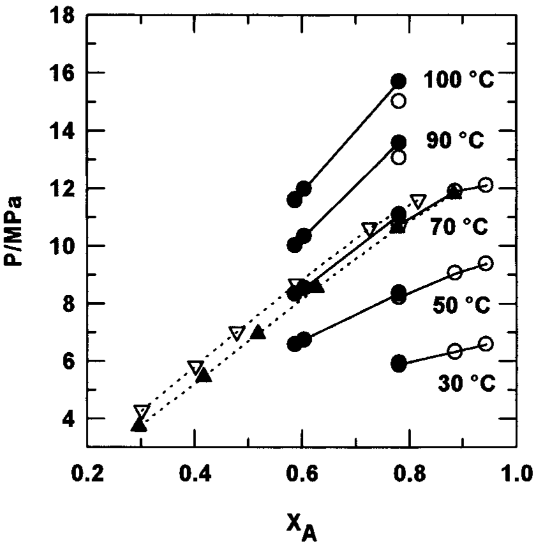

Figure 12. Comparison of vapor−liquid equilibria of carbon dioxide (A) + nonane (B) + cumene (C) with carbon dioxide (A) + nonane (B) and carbon dioxide (A) + cumene (B). Weight % Nonane in Cumene: (▽) 0; (●) 45; (○) 78; (▲) 100.

Conclusions

Vapor−liquid equilibria were measured for mixtures of carbon dioxide with nonane, cumene, propylbenzene, and mesitylene at approximately 70 °C and for propane with nonane, cumene, and mesitylene at approximately 104 °C. The vapor phase compositions for both the carbon dioxide and propane systems were found to be highly related to the volatility of the C_9 component regardless of chemical structure, explaining why previous aromatic/aliphatic separations by supercritical extraction with carbon dioxide and ethane have not proven to be very selective. Additionally, the differences in the phase equilibria of the systems seem to be attributable to the differences in the self-association of the C_9 components.

Acknowledgment

The authors would like to thank Dr. Keith P. Johnston of the University of Texas at Austin for supplying them with the design of the variable−volume batch cell.

Literature Cited

Chou, G. F.; Forbert, R. R.; Prausnitz, J. M. High-Pressure Vapor−Liquid Equilibria for CO_2/*n*-Decane, CO_2/Tetralin, and CO_2/*n*-Decane/Tetralin at 71.1 and 104.4 °C. *J. Chem. Eng. Data* **1990**, , 26−29.

de Haan, A. B.; de Graauw, J. Separation of Alkanes and Aromatics with Supercritical C_2H_6, CO_2, $CClF_3$, and CHF_3. *Sep. Sci. Technol.* **1992**, *27*, 43−60.

Dhalewadikar, S. V.; Seckner, A. J.; McHugh, M. A.; Guckes, T. L. Separation of Dodecane−Biphenyl Mixtures Using Supercritical Ethane, Carbon Dioxide, and Ammonia. *Ind. Eng. Chem. Res.* **1987**, *26*, 976−982.

Hutchenson, K. W.; Roebers, J. R.; Thies, M. C. Vapor−Liquid Equilibrium for Phenanthrene-Toluene Mixtures at Elevated Temperatures and Pressures. *Fluid Phase Equilibria* **1990**, *60*, 309−317.

Jennings, D. W.; Lee, R. J.; Teja, A. S. Vapor−Liquid Equilibria in the Carbon Dioxide + Ethanol and Carbon Dioxide + 1-Butanol Systems. *J. Chem. Eng. Data* **1991**, *36*, 303−307.

Jennings, D. W.; Chang, F.; Bazaan, V.; Teja, A. S. Vapor−Liquid Equilibria for Carbon Dioxide + 1-Pentanol. J. *Chem. Eng. Data* **1992**, *37*, 337−338.

Lemert, R. M.; Fuller, R. A.; Johnston, K. P. Reverse Micelles in Supercritical Fluids. 3. Amino Acid Solubilization in Ethane and Propane. *J. Phys. Chem.* **1990**, *94*, 6021 −6028.

Mawson, S.; Johnston, K. P.; Combes, J. R.; DeSimone, J. M. Formation of Poly(1,1,2,2-tetrahydroperfluorodecyl acrylate) Submicron Fibers and Particles from Supercritical Carbon Dioxide Solutions. *Macromolecules* **1995**, *28*, 3182−3191.

McHugh, M. A.; Seckner, A. J.; Yogan, T. J. High Pressure Phase Behavior of Binary Mixtures of Octacosane and Carbon Dioxide. *Ind. Eng. Chem. Fundam.* **1984**, *23*, 493−499.

Nagarajan, N.; Robinson, R. L., Jr. Equilibrium Phase Compositions, Phase Densities, and Interfacial Tensions for CO_2 + Hydrocarbon Systems. 2 CO_2 + *n*-Decane. *J. Chem. Eng. Data* **1986**, *31*, 168−171.

Occhiogrosso, R. N.; Igel, J. T.; McHugh, M. A. Phase Behavior of Carbon Dioxide-Aromatic Hydrocarbon Mixtures. *Fluid Phase Equilib.* **1986**, *26*, 165−179.

Radosz, M.; Cotterman, R. L.; Prausnitz, J. M. Phase Equilibria in Supercritical Propane Systems for Separation of Continuous Oil Mixtures. *Ind. Eng. Chem. Res.* **1987**, *26*, 731−737.

Reamer, H. H.; Sage, B. H. Phase Equilibria in Hydrocarbon Systems. Volumetric and Phase Behavior of the *n*-Decane−CO_2 System. *J. Chem. Eng. Data* **1963**, *8*, 508 −513.

Reamer, H. H.; Sage, B. H. Phase Equilibria in Hydrocarbon Systems. Volumetric and Phase Behavior of the Propane−*n*-Decane System. *J. Chem. Eng. Data* **1966**, *11*, 17−24.

Reid, R. C.; Prausnitz, J. M.; Poling, B. E. *The Properties of Gases & Liquids*, 4th ed.; McGraw-Hill, Inc.: New York, 1987.

Simnick, J. J.; Lawson, C. C.; Lin, H. M.; Chao, K. C. Vapor−Liquid Equilibrium of the Hydrogen/Tetralin System at Elevated Temperatures and Pressures. *AIChE J.* **1977**, *23*, 469−476.

Thies, M. C.; Paulaitis, M. E. Vapor−Liquid Equilibrium for 1-Methylnaphthalene/Methanol Mixtures at Elevated Temperatures and Pressures. *J. Chem. Eng. Data* **1984**, *29*, 438−440.

Received for review January 29, 1996. Accepted April 28, 1996.[⊗]

JE960033N

[⊗] Abstract published in *Advance ACS Abstracts,* June 1, 1996.